IEEE Access
Multidisciplinary | Rapid Review | Open Access Journal

Received November 14, 2019, accepted November 25, 2019, date of publication November 29, 2019,
date of current version December 23, 2019.

Digital Object Identifier 10.1109/ACCESS.2019.2956818

Adaptive Closed-Loop Control Allocation-Based Fault Tolerant Flight Control for an Overactuated Aircraft

BINWEN LU, JIANJUN MA, (Member, IEEE), AND ZHIQIANG ZHENG
College of Intelligent Science and Technology, National University of Defense Technology, Changsha 410073, China

Corresponding author: Jianjun Ma (jianjunma@hotmail.com)

This work was supported in part by the National Science Foundation of China under Grant 61203095 and Grant 61403407.

ABSTRACT This paper discusses the adaptive control allocation based fault tolerant flight control problem for an overactuated aircraft in the presence of unknown uncertainties and actuator faults. Inspired by the feedback of control moments, an innovative adaptive closed-loop control allocation scheme with an estimator for the uncertainties is designed to tackle the distinct non-monotonic and the coupled nonlinearity caused by actuator failures or faults. Furthermore, since actuator faults will cause difficulty in modeling the aircraft dynamics precisely, an adaptive super twisting sliding mode controller is developed to track the reference trajectory. The convergence of the adaptive closed-loop control allocation and the stability of the fault tolerant flight control system is analyzed. Simulation results indicate the effectiveness and performance of the developed controller.

INDEX TERMS Adaptive, closed-loop control allocation, fault tolerant flight control, super twisting sliding mode, overactuated aircraft.

I. INTRODUCTION

Over the last three decades, the problem of fault tolerant control (FTC) has been intensively studied with the growing demand for safety, reliability and maintainability in modern industrial systems [1], [2]. Various FTC methods have been presented in a wide range of applications such as aircraft, marine vehicles, hypersonic vehicles, and so on [3]–[5]. In particular, the specific operating environment of the flight vehicle is adverse which increases the risk of malfunctions in sensors, actuators, and controllers . What's more, once those components were broken, it is scarcely possible that its hardware can be repaired instantly. Hence, any component or system fault/failure cannot be fixed with replacement parts. Not only these issues may potentially lead to property loss, but also threats of system safety, which has motivated significant research of FTC in aircraft control systems to accommodate or manage failures [6].

Survey papers by [7] and [8] provided excellent overviews of FTC. Generally speaking, FTC techniques can be classified into two types, namely passive and active approaches. In the passive approach, the controller is designed to maintain stability and tolerate only a limited number of previously-known faults. In this case, it can be implemented easily as a fixed controller but has very limited fault tolerance. Active FTC, on the other hand, could be designed for the cases using the available data from both physical and analytic system redundancy to accommodate unanticipated faults. To reconfigure the control law online, the most up-to-date information on the system faults must be provided to refresh the active FTC algorithm. The fault information can be obtained from dedicated fault detection and identification (FDI) system (see, for instance [9], [10]). Therefore, there is no doubt that, to achieve a successful control system reconfiguration in active FTC approaches, a real-time FDI scheme is a significant part [11]–[13]. For the sake of real-time and computational cost, these issues pose challenges to the application of active FTC. One of the effective schemes for handling the actuator fault is disturbance observer-based FTC. In [14], parametric uncertainties, external disturbances, and actuator constraints have been considered for the flexible air-breathing hypersonic vehicle by using a disturbance observer-based fault-tolerant output tracking control. Besides, the nonlinearities of control surface have been got the researcher's attention, in [15] the backlash hysteresis in control surface and the partial loss of effectiveness of actuators and were

The associate editor coordinating the review of this manuscript and approving it for publication was Yonghao Gui.

taken into account. Tracking control with the quantization mechanism was studied in [16] by using an interval type-2 fuzzy neural network.

In over-actuated systems, one existing technique to increase fault tolerance is using a control allocator (CA) that distributes controller command among the redundant healthy actuators [17]. The benefit of CA is that the controller can handle actuator failures in fault situations without reconfiguring the basic control law. There are several methods for solving the allocation problem, e.g. the direct control allocation method, the interior point method, the active set method, the adaptive estimation method etc., which can be found in [18]–[21]. In [22]–[24], a sequential quadratic programming technique is used to cope with the control allocation problem. Reference [25] proposes an adaptive sliding-mode-based control allocation scheme to accommodate actuator faults, which is used to redistribute virtual control signals among the available actuators under faulty conditions. The article [26], a fault-tolerant control scheme with a fixed control allocation strategy is proposed for linear time varying systems, by which the effects of actuator faults in the critical control channels can be compensated and the remaining effects can be minimized. In [27] a real-time control allocation algorithm is devised to deliver control command to position and attitude actuators in proportion to the effectiveness degree of each actuator. In general, most of the CA schemes are designed based on the assumption that the control moments mapping functions of actuators are linear. However, the linear assumption can be hard to satisfy in practice, especially in the case of actuator failures or faults. For the aircraft with multiple control surfaces, the newly imported control surfaces would increase the reliability of the system, meanwhile would generate nonlinearity and coupling in the actuator system significantly. Another general situation is that the faults resulted from control surfaces will drive the actuator system into the nonlinear operation area. The assumption of a linear relationship between the surfaces and control moments can not be held under those conditions. Since the retrieval fails for the desired virtual moments required by the upper basic control law, neglecting the nonlinearities of mapping function would cause degradation or instability of the flight control system.Some researches on this problem have been carried out via adopting nonlinear optimal programming technique [28] and intelligence evolution algorithm [29], [30], nevertheless, adaptive fault tolerant control allocation with considering of non-monotonic nonlinearity of control surfaces remains as a challenge for flight control system design of the overactuated aircraft [31], [32].

This paper investigates the problem of adaptive FTC with consideration of the nonlinear moments mapping function of actuators which focuses mainly on the non-monotonic nonlinearity and the coupled nonlinearity. Considering the adverse effects of FDI model on the rapidity and accuracy of fault-tolerance controller, a novel closed-loop control allocation based nonlinear sliding model adaptive fault-tolerant control scheme is proposed for a class of aircraft system with multiple actuators. The main contributions of this paper include:

(i) In order to compensate the non-monotonic and the coupled nonlinearity of control surfaces, a novel closed-loop adaptive control allocation method based on the moments feedback is developed to calculate the desired actuators' demands with considerable computational cost.

(ii) An adaptive estimator is proposed to estimate the uncertainties of actuators' dynamics caused by faults in the control allocation process, which make the control allocation algorithm more practical by reducing dependence on FDI modules.

(iii) Super-twisting sliding mode control combined with the proposed adaptive closed-loop control allocation can improve the fault tolerant performance of the flight control system of over-actuated aircraft subject to the serious faults of multiple actuators.

The rest of the paper is organized as follows. Section 2 describes the nonlinear FTC problem formulation and the modeling of an overactuated aircraft. Proposed algorithms are given in Section 3. In Section 4, the application of the proposed FTC scheme is illustrated by the case of an overactuated aircraft subject to actuator faults. This is followed by conclusions in Section 5.

II. PROBLEM FORMULATION AND PRELIMINARIES

A. DYNAMICS OF AN OVERACTUATED AIRCRAFT

The nonlinear dynamic model of F-18 aircraft [33] is shown in equation (1). Here Vel is velocity, g_0 is gravitational constant. α, β, ϕ and θ represent the angle of attack, sideslip, roll and pitch respectively. p, q and r are the angular rate of roll, pitch and yaw. α_0 is the trim angle of attack. Also, l, m, n, i, y and z are relevant aerodynamic moment coefficients.

$$\begin{bmatrix} \dot{\alpha} \\ \dot{\beta} \\ \dot{\phi} \\ \dot{\theta} \\ \dot{p} \\ \dot{q} \\ \dot{r} \end{bmatrix} = \begin{bmatrix} q - p\beta + z_\alpha (\alpha - \alpha_0) + \dfrac{g_0}{Vel} (\cos\theta \cos\phi - \cos\theta_0) \\ y_\beta + p (\sin\alpha_0 + \alpha - \alpha_0) - r\cos\alpha_0 + \dfrac{g_0}{Vel} \cos\theta \sin\phi \\ p + q\tan\theta \sin\phi + r\tan\theta \cos\phi \\ q\cos\phi - r\sin\phi \\ l_\beta \beta + l_q q + l_r r + \left(l_{\beta\alpha}\beta + l_{r\alpha} r\right)(\alpha - \alpha_0) + l_p p \\ -i_1 q r m_\alpha (\alpha - \alpha_0) + m_q q + i_2 pr \\ -m_{\dot{\alpha}} \dfrac{g_0}{Vel} (\cos\theta \cos\phi - \cos\theta_0) \\ n_\beta \beta + n_r r + n_p p + n_{p\alpha} p (\alpha - \alpha_0) - i_3 pq + n_q q \end{bmatrix} + \begin{bmatrix} 0 & 0 & 0 \\ 0 & 0 & 0 \\ 0 & 0 & 0 \\ 0 & 0 & 0 \\ 1 & 0 & 0 \\ 0 & 1 & 0 \\ 0 & 0 & 1 \end{bmatrix} v(u) \quad (1)$$

In order to adopt the control allocation technique, a new value $v(u)$ is imported to represent the virtual control signal, then we have

$$\begin{cases} \dot{x}_1 = f_1(x_1, x_3) + g_1(x_1, x_3)x_2 \\ \dot{x}_2 = f_2(x_1, x_2, x_3) + g_2 v(u) \\ \dot{x}_3 = f_3(x_1, x_2, x_3) \\ y = x_1 \end{cases} \tag{2}$$

where $x_1 = \begin{bmatrix} \alpha & \beta & \phi \end{bmatrix}^T$, $x_2 = \begin{bmatrix} p & q & r \end{bmatrix}^T$, $x_3 = \theta$. $v(u) = \begin{bmatrix} L & M & N \end{bmatrix}^T$ represents the control moments in three body axis. $u = \begin{bmatrix} \delta_{le} & \delta_{re} & \delta_{la} & \delta_{ra} & \delta_r & \delta_{lef} & \delta_{tef} \end{bmatrix}^T$ includes seven control effectors consisting of left and right horizontal stabilizers (δ_{le}, δ_{re}), left and right ailerons (δ_{la}, δ_{ra}), leading and trailing edge flaps (δ_{lef}, δ_{ref}), and rudder δ_r. f_1, g_1, f_2 and g_2 in (2) are defined as

$$f_1 = \begin{bmatrix} z_\alpha (\alpha - \alpha_0) + \dfrac{g_0}{Vel} (\cos\theta \cos\phi - \cos\theta_0) \\ y_\beta + \dfrac{g_0}{Vel} \cos\theta \sin\phi \\ 0 \end{bmatrix} \tag{3}$$

$$f_2 = \begin{bmatrix} l_\beta \beta + l_q q + l_r r + l_p p - i_1 qr \\ m_q q + i_2 pr - m_{\dot{\alpha}} \dfrac{g_0}{Vel} (\cos\theta \cos\phi - \cos\theta_0) \\ n_\beta \beta + n_r r + n_p p - i_3 pq + n_q q \end{bmatrix} + \begin{bmatrix} \left(l_{\beta\alpha}\beta + l_{r\alpha} r\right)(\alpha - \alpha_0) \\ m_\alpha (\alpha - \alpha_0) \\ n_{p\alpha} p (\alpha - \alpha_0) \end{bmatrix} \tag{4}$$

$$g_1 = \begin{bmatrix} -\beta & 1 & 0 \\ \sin\alpha_0 + \alpha - \alpha_0 & 0 & -\cos\alpha_0 \\ 1 & \tan\theta \sin\phi & \tan\theta \cos\phi \end{bmatrix} \tag{5}$$

$$g_2 = \begin{bmatrix} 1 & 0 & 0 \\ 0 & 1 & 0 \\ 0 & 0 & 1 \end{bmatrix} \tag{6}$$

In addition, the actuator faults are modeled as:

$$u_c = Ku + \Sigma \bar{u} \tag{7}$$

where u is the input command, $\bar{u}$ is the stuck position if the actuator is locked, and

$$K = diag\left\{k_1, k_2, \cdots, k_i, \cdots, k_p\right\} \tag{8}$$

$$\Sigma = diag\left\{\frac{\varepsilon}{k_1 + \varepsilon}, \frac{\varepsilon}{k_2 + \varepsilon}, \cdots, \frac{\varepsilon}{k_p + \varepsilon}\right\} \tag{9}$$

where $k_i \in [0, 1]$ represents the efficiency coefficient of actuator u_i, ε is a small positive number and satisfies $0 < \varepsilon \ll 1$.

B. PRELIMINARIES

In order to design fault-tolerant control laws, we introduce the following lemma.

Lemma 1: Considering the following system:

$$\dot{x} = u \tag{10}$$

There exists a range of arbitrary positive constants λ and τ such that the sliding variable $x(t)$ and its derivative $\dot{x}(t)$ converge to the zero in finite time if the super twisting sliding mode control law is designed as (11).

$$\begin{cases} u = -\lambda |x|^{\frac{1}{2}} \operatorname{sgn}(x) + \rho \\ \dot{\rho} = -\tau \operatorname{sgn}(x) \end{cases} \tag{11}$$

Proof: First of all, we set

$$A = \begin{bmatrix} -\dfrac{1}{2}\lambda & \dfrac{1}{2} \\ -\tau & 0 \end{bmatrix}$$

with $\lambda > 0$ and $\tau > 0$, then the characteristic polynomial of A is described as $p(s) = s^2 + \frac{1}{2}\lambda s + \frac{1}{2}\tau$, and A is Hurwitz matrix. For an arbitrary positive definite symmetric matrix Q, there must be a positive definite symmetric matrix P satisfying the Lyapunov equation $A^T P + PA = -Q$.

Consider the quadratic function as the Lyapunov equation: $V(x) = \eta^T P \eta$ with $\eta^T = \begin{bmatrix} \operatorname{sgn}(x)|x|^{\frac{1}{2}} & \rho \end{bmatrix}$. The $V(x)$ is positive definite and differentiable.

Considering the equation $\dfrac{d\,|x|}{dt} = \dot{x} \operatorname{sgn}(x)$, the derivative of η can be calculated:

$$\begin{cases} \dot{\eta}_1 = \dfrac{1}{2|x|^{\frac{1}{2}}} \left(-\lambda |x|^{\frac{1}{2}} sgn(x) + \rho\right) \\ \dot{\eta}_2 = -\tau sgn(x) \end{cases} \tag{12}$$

Then, the consequence can be obtained:

$$\dot{\eta} = \frac{1}{|x|^{\frac{1}{2}}} A\eta \tag{13}$$

The derivative of the Lyapunov function candidate is:

$$\begin{aligned} \dot{V}(x) &= \frac{1}{|x|^{\frac{1}{2}}} \eta^T \left(A^T P + PA\right) \eta \\ &= -\frac{1}{|x|^{\frac{1}{2}}} \eta^T Q \eta \\ &= -W \end{aligned} \tag{14}$$

where W is a positive constant. The $\dot{V}(x)$ is negative definite which means that the system (10) is asymptotic stable under the designed controller. Since $V(x)$ is quadratic positive definite, we have:

$$\lambda_{\min}(P) \|\eta\|_2^2 \leqslant V(x, y) \leqslant \lambda_{\max}(P) \|\eta\|_2^2 \tag{15}$$

where $\lambda_{\min}(P)$ and $\lambda_{\max}(P)$ are the minimum and maximum eigenvalue of P, $||\cdot||$ represents the Euclidean norm, then $\|\eta\|_2^2 = \eta_1^2 + \eta_2^2 = |x| + \rho^2$. Furthermore, we can obtain:

$$|\eta_1| = |x|^{\frac{1}{2}} \leqslant \|\eta\|_2 \leqslant \frac{V^{\frac{1}{2}}}{\lambda_{\min}^{\frac{1}{2}}(P)} \tag{16}$$

and

$$\begin{aligned} \dot{V} &\leqslant -\frac{1}{|x|^{\frac{1}{2}}} \lambda_{\min}(Q) \|\eta\|_2^2 \\ &= -\frac{\|\eta\|_2}{|\eta_1|} \lambda_{\min}(Q) \|\eta\|_2 \\ &\leqslant -\lambda_{\min}(Q) \|\eta\|_2 \end{aligned} \tag{17}$$

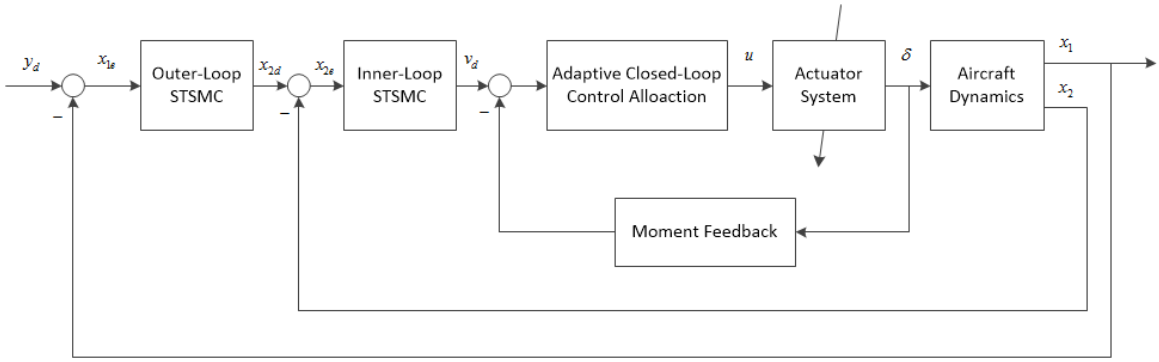

FIGURE 1. The structure diagram of proposed nonlinear FTC control scheme.

Consider

$$\frac{V^{\frac{1}{2}}}{\lambda_{\min}^{\frac{1}{2}}(P)} \leqslant \|\eta\|_2 \tag{18}$$

Then, we have

$$\dot{V} \leqslant -\gamma(Q)V^{\frac{1}{2}}(x) \tag{19}$$

where $\gamma(Q) = \lambda_{\min}(Q)\lambda_{\max}^{-\frac{1}{2}}(P)$. Based on the well-known Lyapunov stability theorem for finite-time convergence [34], [35], we conclude that the sliding variable and its derivative can be derived to zero in finite time.

It means that the sliding variable and its derivative can be derived to zero in finite time. The convergence time can be computed from:

$$t \leqslant T = \frac{2}{\gamma(Q)}V^{\frac{1}{2}}(x_0) \tag{20}$$

where $Q = I$, P is calculated through:

$$P = \begin{bmatrix} \dfrac{2\tau+1}{\lambda} & -1 \\ -1 & \dfrac{\lambda^2+2\tau+1}{2\lambda\tau} \end{bmatrix} \tag{21}$$

III. FAULT TOLERANT FLIGHT CONTROL DESIGN

The control objective is to design an adaptive nonlinear fault tolerant control strategy such that system output could asymptotically track the desired trajectory in the presence of actuator faults. To facilitate control laws design, we put forward the following assumptions and preliminaries.

Assumption 1: The aircraft system is in cruising flying, with known steady velocity.

Assumption 2: The desired trajectory $y_d(t)$ is a known bounded function of time, with known bounded derivatives.

Assumption 3: The state $x(t)$ of the system is available for measurement.

In this section, a nonlinear fault tolerant flight control based on adaptive closed-loop control allocation and super twisting sliding mode control is designed. The system's stability is analyzed. The structure diagram of proposed control scheme is show in figure 1.

A. SUPER-TWISTING SLIDING MODE CONTROL DESIGN

Sliding mode control (SMC) is widely used in control system design owing to its good performance, such as robustness, fast response, good transient performance and so on [36]. In this section, super-twisting sliding mode control (STSMC) is designed to acquire the nominal virtual control signal $v(u)$. The control target is to drive the sliding variable and its derivative to zero in finite time. The system is divided into the outer-loop subsystem and the inner-loop subsystem. Define the desired signals $y_d = \begin{bmatrix} \alpha_d & \beta_d & \phi_d \end{bmatrix}$ and the tracking error $y_e = y - y_d = x_1 - y_d$. The dynamic of tracking error system can be described as:

$$\dot{y}_e = -\dot{y}_d + f_1(x_1, x_2) + g_1(x_1, x_3)x_2 \tag{22}$$

where x_2 is the control signal in the out-loop of the aircraft system.

We design the outer-loop STSMC control laws as:

$$\begin{cases} x_{2d} = g_1^{-1}(\dot{y}_d - f_1 - \lambda_1|y_e|^{\frac{1}{2}}\,\mathrm{sgn}(y_e) + \rho_1) \\ \dot{\rho}_1 = -\tau\,\mathrm{sgn}(y_e) \end{cases} \tag{23}$$

where $\lambda_1 \in R_+^{3\times1}$ and $\tau_1 \in R_+^{3\times1}$ are the designed positive constant gains vectors. $\mathrm{sgn}(y_e)$ is the sign function of y_e .

Substituting the control law (23) to (22), the system's state equation is transformed to

$$\begin{cases} \dot{x}_{1e} = -\lambda_1|x_{1e}|^{\frac{1}{2}}\,\mathrm{sgn}(x_{1e}) + \rho_1 \\ \dot{\rho}_1 = -\tau_1\,\mathrm{sgn}(x_{1e}) \end{cases} \tag{24}$$

where $x_{1e} = y_e = x_1 - y_d$.

According to Lemma 1, the error of the outer-loop subsystem will converge to zero in finite time. Furthermore, let $x_{2e} = x_2 - x_{2d} = \begin{bmatrix} p_e & q_e & r_e \end{bmatrix}^T$, the error dynamic of inner-loop subsystem is transformed to:

$$\dot{x}_{2e} = -\dot{x}_{2d} + f_2(x_1, x_2, x_3) + g_2 v(u) \tag{25}$$

where $\dot{x}_{2d}$ can be achieved through a first-order filter by introducing a new variable x_{2c} [37], [38].

$$t_\omega \dot{x}_{2c} + x_{2c} = x_{2d}, \quad x_{2c}(0) = x_{2d}(0) \tag{26}$$

where t_ω is the time constant. Because v is used as the control signal of the inner loop, the inner-loop SMC control laws v_d

is designed as:

$$\begin{cases} v_d = g_2^{-1}\left(\dot{x}_{2c} - f_2 - \lambda_2 |x_{2e}|^{\frac{1}{2}} \operatorname{sgn}(x_{2e}) + \rho_2\right) \\ \dot{\rho}_2 = -\tau_2 \operatorname{sgn}(x_{2e}) \end{cases} \tag{27}$$

where $\lambda_2 = \begin{bmatrix} \lambda_{21} & \lambda_{22} & \lambda_{23} \end{bmatrix}^T$ and $\tau_2 = \begin{bmatrix} \tau_{21} & \tau_{22} & \tau_{23} \end{bmatrix}^T$ are designed parameters.

Consider the Lyapunov function of the inner-loop system as:

$$V_0 = \eta_{2e}^T M \eta_{2e} \tag{28}$$

with $\eta_{2e}^T = \begin{bmatrix} \kappa_1^T & \kappa_2^T \end{bmatrix}^T = \begin{bmatrix} \operatorname{sgn}(x_{2e})|x_{2e}|^{\frac{1}{2}} & \rho_2 \end{bmatrix}$

Define

$$P_1 = \begin{bmatrix} a_1 & b_1 \\ c_1 & d_1 \end{bmatrix} = \begin{bmatrix} \dfrac{2\tau_{21}+1}{\lambda_{21}} & -1 \\ -1 & \dfrac{\lambda_{21}^2 + 2\tau_{21} + 1}{2\lambda_{21}\tau_{21}} \end{bmatrix} \tag{29}$$

$$P_2 = \begin{bmatrix} a_2 & b_2 \\ c_2 & d_2 \end{bmatrix} = \begin{bmatrix} \dfrac{2\tau_{22}+1}{\lambda_{22}} & -1 \\ -1 & \dfrac{\lambda_{22}^2 + 2\tau_{22} + 1}{2\lambda_{22}\tau_{22}} \end{bmatrix} \tag{30}$$

$$P_3 = \begin{bmatrix} a_3 & b_3 \\ c_3 & d_3 \end{bmatrix} = \begin{bmatrix} \dfrac{2\tau_{23}+1}{\lambda_{23}} & -1 \\ -1 & \dfrac{\lambda_{23}^2 + 2\tau_{23} + 1}{2\lambda_{23}\tau_{23}} \end{bmatrix} \tag{31}$$

Then, M can be obtained as:

$$M = \begin{bmatrix} a_1 & b_1 & 0 & 0 & 0 & 0 \\ 0 & 0 & a_2 & b_2 & 0 & 0 \\ 0 & 0 & 0 & 0 & a_3 & b_3 \\ c_1 & d_1 & 0 & 0 & 0 & 0 \\ 0 & 0 & c_2 & d_2 & 0 & 0 \\ 0 & 0 & 0 & 0 & c_3 & d_3 \end{bmatrix} \tag{32}$$

Based on the above discussion, we have:

$$\begin{aligned} V_0 &= \eta_{2e}^T M \eta_{2e} \\ &= \begin{bmatrix} \kappa_{11} & \kappa_{21} \end{bmatrix}^T P_1 \begin{bmatrix} \kappa_{11} & \kappa_{21} \end{bmatrix} \\ &\quad + \begin{bmatrix} \kappa_{12} & \kappa_{22} \end{bmatrix}^T P_2 \begin{bmatrix} \kappa_{12} & \kappa_{22} \end{bmatrix} \\ &\quad + \begin{bmatrix} \kappa_{13} & \kappa_{23} \end{bmatrix}^T P_3 \begin{bmatrix} \kappa_{13} & \kappa_{23} \end{bmatrix} \\ &= a_1\kappa_{11}^2 + c_1\kappa_{11}\kappa_{21} + b_1\kappa_{11}\kappa_{21} + d_1\kappa_{21}^2 \\ &\quad + a_2\kappa_{12}^2 + c_1\kappa_{12}\kappa_{22} + b_2\kappa_{12}\kappa_{22} + d_2\kappa_{22}^2 \\ &\quad + a_3\kappa_{13}^2 + c_3\kappa_{13}\kappa_{23} + b_3\kappa_{13}\kappa_{23} + d_3\kappa_{23}^2 \end{aligned} \tag{33}$$

Define

$$A_1 = \begin{bmatrix} -\dfrac{1}{2}\lambda_{21} & \dfrac{1}{2} \\ -\tau_{21} & 0 \end{bmatrix} \tag{34}$$

$$A_2 = \begin{bmatrix} -\dfrac{1}{2}\lambda_{22} & \dfrac{1}{2} \\ -\tau_{22} & 0 \end{bmatrix} \tag{35}$$

$$A_3 = \begin{bmatrix} -\dfrac{1}{2}\lambda_{23} & \dfrac{1}{2} \\ -\tau_{23} & 0 \end{bmatrix} \tag{36}$$

Then, we can have

$$\begin{aligned} \dot{V}_0 &= \begin{bmatrix} \kappa_{11} & \kappa_{21} \end{bmatrix}^T \left(A_1^T P_1 + P_1 A_1\right) \begin{bmatrix} \kappa_{11} & \kappa_{21} \end{bmatrix} \\ &\quad + \begin{bmatrix} \kappa_{12} & \kappa_{22} \end{bmatrix}^T \left(A_2^T P_2 + P_2 A_2\right) \begin{bmatrix} \kappa_{12} & \kappa_{22} \end{bmatrix} \\ &\quad + \begin{bmatrix} \kappa_{13} & \kappa_{23} \end{bmatrix}^T \left(A_3^T P_3 + P_3 A_3\right) \begin{bmatrix} \kappa_{13} & \kappa_{23} \end{bmatrix} \\ &= -\begin{bmatrix} \kappa_{11} & \kappa_{21} \end{bmatrix}^T \begin{bmatrix} \kappa_{11} & \kappa_{21} \end{bmatrix} \\ &\quad - \begin{bmatrix} \kappa_{12} & \kappa_{22} \end{bmatrix}^T \begin{bmatrix} \kappa_{12} & \kappa_{22} \end{bmatrix} \\ &\quad - \begin{bmatrix} \kappa_{13} & \kappa_{23} \end{bmatrix}^T \begin{bmatrix} \kappa_{13} & \kappa_{23} \end{bmatrix} \\ &\leqslant -W_0 \end{aligned} \tag{37}$$

where W_0 is a positive constant. According to Lemma 1, the error of the inner-loop subsystem will converge to zero in finite time.

B. DESIGN OF ADAPTIVE CLOSED-LOOP CONTROL ALLOCATION

The categories of nonlinearities encountered in actuator mainly include monotonic nonlinearity, non-monotonic nonlinearity and coupled nonlinearity. Most of the solutions are obtained by using quadratic programming, nonlinear programming and intelligence method, and so on. Against the deficiencies such as large computational cost and poor real-time performance, a new control allocation scheme based on control surface nonlinear feedback is adopted. Firstly, build the mapping function between control surface u and control moment $v(u)$.

$$v(u) = (B + \Phi(u))\, u \tag{38}$$

where $v(u) = \begin{bmatrix} L & M & N \end{bmatrix}^T$. L, M and N denote the roll, pitch and yaw control moment respectively. $B \in R^{3\times 7}$ represents the linear part of mapping function, $\Phi(u)$ implies the nonlinear part which is defined as follows [39].

$$\Phi(u) = \frac{1}{2}\begin{bmatrix} u^T C_l \\ u^T C_m \\ u^T C_n \end{bmatrix} \tag{39}$$

with

$$C_l = \begin{bmatrix} 2\dfrac{\partial^2 L}{\partial u_1^2} & \dfrac{\partial^2 L}{\partial u_1 \partial u_2} & \cdots & \dfrac{\partial^2 L}{\partial u_1 \partial u_p} \\ \dfrac{\partial^2 L}{\partial u_2 \partial u_1} & 2\dfrac{\partial^2 L}{\partial u_2^2} & \cdots & \dfrac{\partial^2 L}{\partial u_2 \partial u_p} \\ \vdots & \vdots & \ddots & \vdots \\ \dfrac{\partial^2 L}{\partial u_p \partial u_1} & \dfrac{\partial^2 L}{\partial u_p \partial u_2} & \cdots & 2\dfrac{\partial^2 L}{\partial u_p^2} \end{bmatrix} \tag{40}$$

$$C_m = \begin{bmatrix} 2\dfrac{\partial^2 M}{\partial u_1^2} & \dfrac{\partial^2 M}{\partial u_1 \partial u_2} & \cdots & \dfrac{\partial^2 M}{\partial u_1 \partial u_p} \\ \dfrac{\partial^2 M}{\partial u_2 \partial u_1} & 2\dfrac{\partial^2 M}{\partial u_2^2} & \cdots & \dfrac{\partial^2 M}{\partial u_2 \partial u_p} \\ \vdots & \vdots & \ddots & \vdots \\ \dfrac{\partial^2 M}{\partial u_p \partial u_1} & \dfrac{\partial^2 M}{\partial u_p \partial u_2} & \cdots & 2\dfrac{\partial^2 M}{\partial u_p^2} \end{bmatrix} \tag{41}$$

$$C_n = \begin{bmatrix} 2\frac{\partial^2 N}{\partial u_1^2} & \frac{\partial^2 N}{\partial u_1 \partial u_2} & \cdots & \frac{\partial^2 N}{\partial u_1 \partial u_p} \\ \frac{\partial^2 N}{\partial u_2 \partial u_1} & 2\frac{\partial^2 N}{\partial u_2^2} & \cdots & \frac{\partial^2 N}{\partial u_2 \partial u_p} \\ \vdots & \vdots & \ddots & \vdots \\ \frac{\partial^2 N}{\partial u_p \partial u_1} & \frac{\partial^2 N}{\partial u_p \partial u_2} & \cdots & 2\frac{\partial^2 L}{\partial u_p^2} \end{bmatrix} \quad (42)$$

The diagonal elements represent non-monotonic nonlinearity and the others are coupled nonlinearity in C_l, C_m and C_n. The moment mapping function can be described at k sample time as:

$$v(k) = (B + \Phi(k))\, u(k) \quad (43)$$

Then

$$u(k) = B^+ (v_d - \Phi(k)u(k)) \quad (44)$$

where v_d is the desired control moment. Since the part of nonlinearity $\Phi(k)u(k)$ is unknown, design the output of control allocation as follow:

$$u(k) = B^+ (v_d - \Phi(k-1)u(k-1)) \quad (45)$$

Lemma 2: For the nonlinear control allocation system (42), there exist a solution $u(k)$ calculated by (44) such that the error of the control allocation module would converge to a bounded region around zero.

In order to explain the Lemma 2, we define the discrete dynamic system as:

$$x(k+1) = f(k, x(k)) \quad (46)$$

where $x \in R^n, f \in C[N^+ \times R^n, m]$, N^+ is the nonnegative integer set. Set $f(k, 0) = 0,\ \forall k \in N^+$ and assume that the origin is the only equilibrium point. $x(k, k_0, x_0)$ is the solution of the system passing initial point (k_0, x_0). Define $V(k, x) \in C[N^+ \times R^n, R^+]$. The differential of $V(k, x)$ along the system is defined as:

$$\begin{aligned} \Delta V(k, x(k)) &\triangleq V(k+1, x(k+1)) - V(k, x(k)) \\ &= V(k+1, f(k, x(k)) - V(k, x(k)) \end{aligned} \quad (47)$$

Define K function $\Gamma(\cdot) : R_{\geq 0} \to R_{\geq 0}$ as a strictly monotonically increasing continuous function and $\Gamma(0) = 0$. According to [40], if there exist K function $\Gamma(\cdot)$ and the constant $\sigma > 0$ independent of k_0 such that the following inequality (48) hold, then the system's equilibrium point $x = 0$ is uniform stable.

$$\|x(k)\| \leq \Gamma(\|x(k_0)\|), \quad \forall k \geq k_0 \geq 0,\ \forall \|x(k_0)\| < \sigma \quad (48)$$

Based on the above discussion, the convergence of the proposed nonlinear control allocation scheme can be provided. When the desired control moment $v_d = 0$, the following equation is obtained.

$$u(k) = B^{-1}(-\Phi(k-1)u(k-1)) \quad (49)$$

It will be seen that the equilibrium point of the system is $u(k) = 0$. Constructing K function as $\Gamma(\|u(k)\|) = \|u(k)\|$. Because $u(k)$ is bounded, there is constants $\sigma > 0$ independent of k_0 makes the following condition valid.

$$\|u(k)\| \leq \Gamma(\|u(k_0)\|), \quad \forall k \geq k_0 \geq 0,\ \forall \|u(k_0)\| < \sigma \quad (50)$$

Thus the proposed nonlinear control allocation scheme based on moment feedback is uniform stable at the system's equilibrium point $u(k) = 0$.

Substitute (45) to (43), the real control moment is computed as:

$$\begin{aligned} v(k) &= BB^+ (v_d - \Phi(k-1)u(k-1)) + \Phi(k)u(k) \\ &= v_d - \Phi(k-1)u(k-1) + \Phi(k)u(k) \end{aligned} \quad (51)$$

Then, the error $v_e(k)$ can be obtained:

$$v_e(k) = v(k) - v_d = \Phi(k)u(k) - \Phi(k-1)u(k-1) \quad (52)$$

Since the inner loop subsystem is finite time stable according to (37), we know that the difference between $u(k)$ and $u(k-1)$ will converge to a small bounded region, then we have $\lim_{k\to\infty} |u(k) - u(k-1)| \leq \epsilon$ with ϵ a small positive constant. Meanwhile, consider

$$\Phi(k) = \frac{1}{2}\begin{bmatrix} u^T(k)C_l \\ u^T(k)C_m \\ u^T(k)C_n \end{bmatrix} \quad \text{and}$$

$$\Phi(k-1) = \frac{1}{2}\begin{bmatrix} u^T(k-1)C_l \\ u^T(k-1)C_m \\ u^T(k-1)C_n \end{bmatrix},$$

we conclude that the errors of control allocation $v_e(k)$ will converge to a bounded region around zero.

Furthermore, in order to handle the uncertainties caused by the nonlinear feedback, an adaptive method is introduced to compensation, which makes the control allocation more practical. Consider the linear part of control moment as:

$$v_{lin} = v_d - v_{non} \quad (53)$$

where $v_{non} \triangleq \Phi(k-1)u(k-1)$. The real mapping function of linear control moment is described as:

$$v_{lin} = B\Lambda u \quad (54)$$

here $\Lambda \in R^{m\times m}$ is an unknown diagonal matrix, $\Lambda_{ii} \geqslant 0$, representing the impacts of nonlinear feedback and actuator faults. Under this situation, u is acquired as

$$u = (B\Lambda)^{-1} v_{lin} \quad (55)$$

The stabilizing control allocation matrix is computed directly instead of the estimation of Λ, we have

$$u = u_n + u_a = B^+ v_{lin} + \hat{\Delta} v_{lin} \quad (56)$$

where $\hat{\Delta} \in R^{m\times 3}$ is the estimation of the desire matrix Δ which meets the condition:

$$B\Lambda\left(B^+ + \Delta\right) = I \quad (57)$$

Remark 1: Δ compensates the influences of nonlinear feedback and actuator malfunctions. Without an external FDI module, the information of actuator faults is acquired by the adaptive estimation of $\hat{\Delta}$.

Define $\tilde{\Delta} = \hat{\Delta} - \Delta$, consider the condition (53) and (54), the error of control allocation is calculated as:

$$\begin{aligned}\tilde{v} &= v_{lin} - B\Lambda u \\ &= v_{lin} - B\Lambda\left(B^{+} + \hat{\Delta}\right) v_{lin} \\ &= v_{lin} - B\Lambda\left(B^{+} + \Delta + \tilde{\Delta}\right) v_{lin} \\ &= -B\Lambda\tilde{\Delta} v_{lin}\end{aligned} \tag{58}$$

Then, the time derivative of $V_0(x)$ can be obtained:

$$\begin{aligned}\dot{V}_0 &= \frac{\partial V_0}{\partial t} + \frac{\partial V}{\partial x}\left(f_2(t,x) + g_2(v_{non} + v_{lin} - \tilde{v})\right) \\ &\leqslant -W_0 - \frac{\partial V_0}{\partial x} g_2 \tilde{v} \\ &= -W_0 + \frac{\partial V_0}{\partial x} g_2 B\Lambda\tilde{\Delta} v_{lin}\end{aligned} \tag{59}$$

We design the adaptive law:

$$\dot{\hat{\Delta}} = \gamma \mathrm{Proj}_R\left(\hat{\Delta}, -\left(v_{lin}\frac{\partial V_0}{\partial x} g_2 B\right)^T\right) \tag{60}$$

where γ is a gain constant, $\mathrm{Proj}_R(\cdot)$ is a row projection operator defined as:

$$\begin{aligned}\mathrm{Proj}_R(C, Y) &= \mathrm{Proj}_R\left(\begin{bmatrix} c_1^T \\ \vdots \\ c_m^T \end{bmatrix}, \begin{bmatrix} y_1^T \\ \vdots \\ y_m^T \end{bmatrix}\right) \\ &= \begin{bmatrix} \mathrm{Proj}(c_1, y_1)^T \\ \vdots \\ \mathrm{Proj}(c_m, y_m)^T \end{bmatrix}\end{aligned} \tag{61}$$

where $\mathrm{Proj}(\cdot)$ is the projection operator and c_i^T, y_i^T are the ith rows of C and Y, respectively. Recall that for any vector y_i it holds.

$$\tilde{\Delta}_i^T\left(\mathrm{Proj}(\hat{\Delta}_i, y_i) - y_i\right) \leqslant 0 \tag{62}$$

$\tilde{\Delta}_i$ and $\hat{\Delta}_i$ are the i-th rows of $\tilde{\Delta}$ and $\hat{\Delta}$. Refer to $tr(C^T Y) = \sum_{i=1}^{m} c_i^T y_i$, we can obtain:

$$\begin{aligned}&tr\left(\tilde{\Delta}\left(\mathrm{Proj}(\hat{\Delta}, Y) - Y\right)^T \Lambda\right) \\ &\qquad = \sum_{i=1}^{m} \Lambda_{ii}\tilde{\Delta}_i^T\left(\mathrm{Proj}(\hat{\Delta}_i, y_i) - y_i\right) \leqslant 0\end{aligned} \tag{63}$$

In addition, on the basis of (33), the partial derivative of V_0 to x can be calculated as:

$$\frac{\partial V_0}{\partial x} = \begin{bmatrix} \dfrac{a_1\kappa_{11}}{\dfrac{1}{|p_e|^{\frac{1}{2}}}} + (c_1\kappa_{21} + b_1\kappa_{21})\dfrac{1}{2|p_e|^{\frac{1}{2}}} \\ \dfrac{a_2\kappa_{12}}{\dfrac{1}{|q_e|^{\frac{1}{2}}}} + (c_2\kappa_{22} + b_2\kappa_{22})\dfrac{1}{2|q_e|^{\frac{1}{2}}} \\ \dfrac{a_3\kappa_{13}}{\dfrac{1}{|r_e|^{\frac{1}{2}}}} + (c_3\kappa_{23} + b_3\kappa_{23})\dfrac{1}{2|r_e|^{\frac{1}{2}}} \end{bmatrix} \tag{64}$$

C. MAIN RESULT

The above design procedure can be summarized in the following theorem.

Theorem 1: Consider the adaptive closed-loop control allocation based on (45) and (60), which integrated with the super-twisting sliding mode controller (23) and (27), the proposed nonlinear FTC scheme guarantees the system (1) asymptotic stability in the presence of actuator malfunctions.

Proof: Consider the Lyapunov function:

$$V_{ad} = V_0(x) + \frac{1}{2\gamma} tr\left(\tilde{\Delta}\tilde{\Delta}^T\Lambda\right) \tag{65}$$

Based on the above discussion, we can obtain:

$$\begin{aligned}\dot{V}_{ad} &= \dot{V}_0(x) + \frac{1}{\gamma} tr(\tilde{\dot{\Delta}}\tilde{\Delta}^T\Lambda) \\ &= \frac{\partial V_0}{\partial t} + \frac{\partial V_0}{\partial x}\left(f_2(t,x) + g_2(v_{non} + v_{lin} - \tilde{v})\right) \\ &\quad + tr\left(\gamma^{-1}\tilde{\Delta}\dot{\tilde{\Delta}}^T\Lambda\right)\end{aligned} \tag{66}$$

Substituting into, we have:

$$\dot{V}_{ad} \leqslant -W_0 + \frac{\partial V_0}{\partial x} g_2 B\Lambda\tilde{\Delta} v_{lin} + tr\left(\gamma^{-1}\tilde{\Delta}\dot{\tilde{\Delta}}^T\Lambda\right) \tag{67}$$

Furthermore, we will obtain:

$$\begin{aligned}\dot{V}_{ad} &\leqslant -W_0 + tr\left(\tilde{\Delta}\left(v_{lin}\frac{\partial V_0}{\partial x} g_2 B + \gamma^{-1}\dot{\tilde{\Delta}}^T\right)\Lambda\right) \\ &\leqslant -W_0\end{aligned} \tag{68}$$

Therefore, the stability of the closed-loop system with the proposed control is proven.

Remark 2: From Theorem 1 we know that, although there is no external FDI module, the system with actuator faults can remain stable by using the proposed nonlinear adaptive FTC scheme with appropriate selection of the design parameters. Adaptive gain γ is the key parameter to determine the performance of nonlinear FTC system. With the increase of γ, the response of fault-tolerant control system will be faster, but the frequency and control quantity of control signal will also increase, which will lead to an increase of overshoot in the system transition process.

From equations (56), (60) and (64), it can be seen that the compensation signal of adaptive fault-tolerant control u_a is

TABLE 1. Position limits of the control surfaces.

Surface	Upper limit(deg)	Lower limit(deg)
$Horizontaltails$	10.5	-24
$Ailerons$	45	-25
$Leadingedgeflap$	33	-3
$Trailingedgeflap$	45	-8
$Rudder$	30	-30

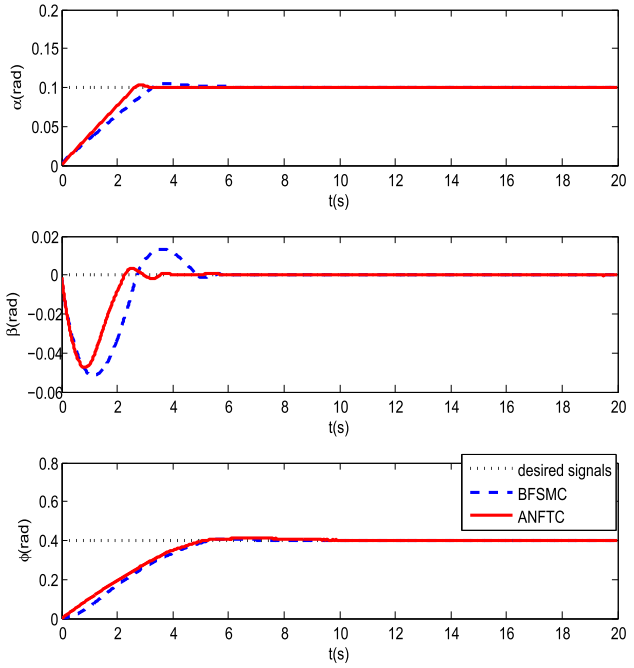

FIGURE 2. Output responses from the BFSMC method (dashed lines) and ANFTC method (solid lines) in normal case.

related to x_{2e} and $sgn(x_{2e})$, which is similar to the structure of switching control term of traditional sliding mode control [41]. One of the disadvantages of this adaptive structure is that it is easy to fall into overestimation the parameters, which may lead to the chattering of control signals. In order to eliminate the overestimation, the transient performances and fault tolerance abilities of the system are compromised in the process of setting control parameters, and the adaptive parameter γ is designed in the form of a saturation function.

$$\gamma = sat(\mu, y_e) = \begin{cases} \gamma_0, & \|y_e\|_\infty \geq \mu \\ \gamma_0 \cdot \dfrac{\|y_e\|_\infty}{\mu}, & \|y_e\|_\infty < \mu \end{cases} \tag{69}$$

where γ_0 is a positive constant, μ is the boundary layer. This adaptive scheme can gradually cease the behavior of adaptation as the system reaches the desired trajectory.

IV. NUMERICAL SIMULATION

In this section, the nonlinear dynamic model of F-18 aircraft is used to verify the effectiveness of the proposed nonlinear adaptive FTC approach. The model of $v(u)$ is nonlinearly

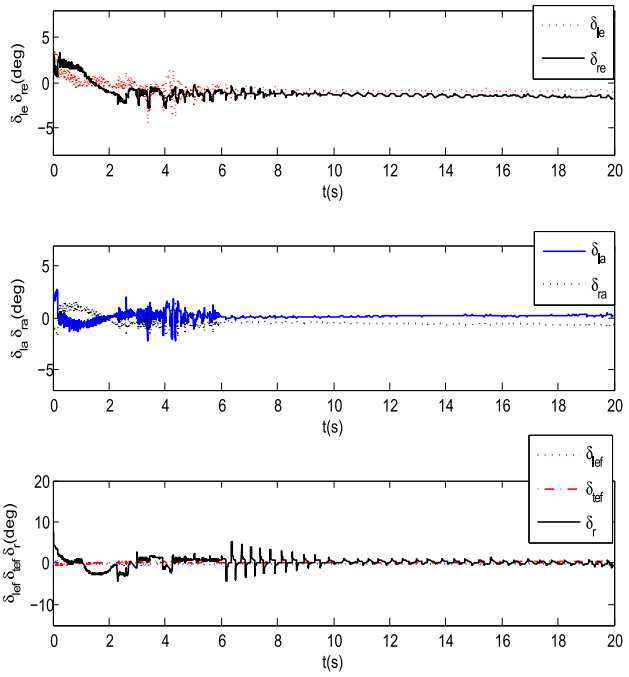

FIGURE 3. Control surfaces deflection signals adopting ANFTC in normal case.

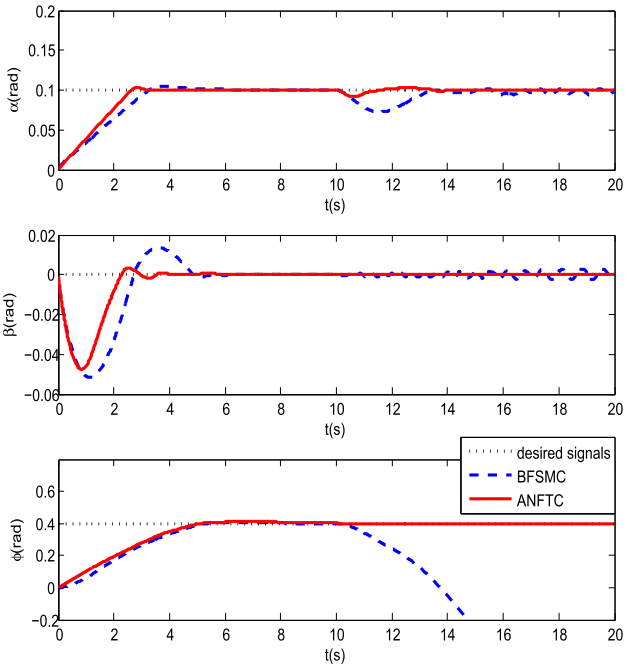

FIGURE 4. Output responses from the BFSMC method (dashed lines) and ANFTC method (solid lines): δ_{re} and δ_{la} are floating at 10s.

fitted by aerodynamic data [42]. The position limits of the control surfaces are given in table 1.

The task given to the proposed adaptive FTC system is to track angle-of-attack and roll angle reference signals while the side-slip angle is regulated to zero.

For comparison purposes, two types of nonlinear controller designs are carried out. The first design is the basic

TABLE 2. The parameters used in simulations.

	Parameters	Values
Control condition	Initial errors	$\alpha_e = -0.1rad$, $\beta_e = 0rad$, $\phi_e = -0.4rad$
	Initial states	$\alpha_{ini} = 0rad$, $\beta_{ini} = 0rad$, $\phi_{ini} = -0.4rad$
	Reference signal	$\alpha_d = 0.1rad$, $\beta_d = 0rad$, $\phi_d = 0.4rad$
Control parameters	SMC	$\lambda_1 = \begin{bmatrix}0.06 & 0.05 & 0.17\end{bmatrix}^T$, $\tau_1 = \begin{bmatrix}0.003 & 0.001 & 0.005\end{bmatrix}^T$ $\lambda_2 = \begin{bmatrix}0.6 & 0.5 & 0.3\end{bmatrix}^T$, $\tau_2 = \begin{bmatrix}0.01 & 0.01 & 0.005\end{bmatrix}^T$ $t_\omega = 0.05$
	Adaptive gain	$\mu = 0.02$ $\gamma = sat(x_e, \mu) = \begin{cases} 0.1, & \|y_e\|_\infty \geq \mu \\ 0.1 \times \frac{\|y_e\|_\infty}{\mu}, & \|y_e\|_\infty < \mu \end{cases}$

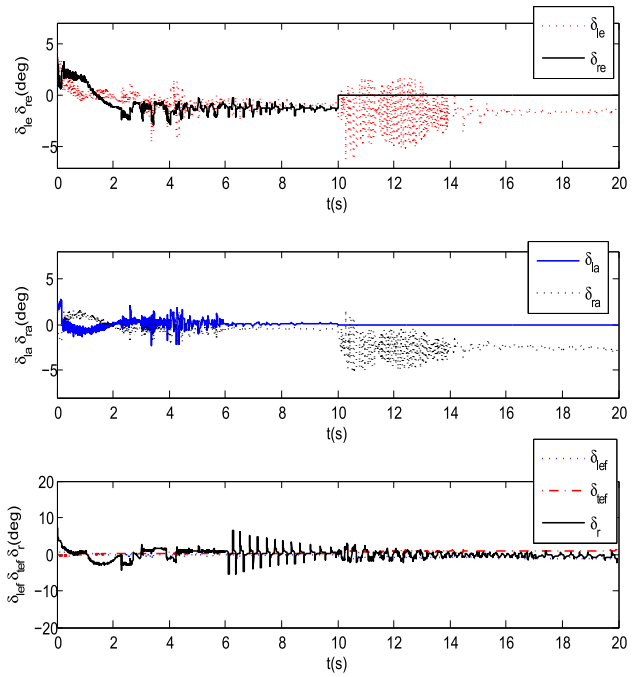

FIGURE 5. Control surfaces deflection signals adopting ANFTC : δ_{re} and δ_{la} are floating at 10s.

nonlinear feedback sliding mode control scheme without adaptive closed-loop control allocation (BFSMC). The second is the adaptive nonlinear FTC with closed-loop control allocation (ANFTC) design proposed in this paper.The above two controllers have the same control parameters of λ_1, τ_1, λ_2, τ_2 and t_ω . The parameters used in simulations are listed in table 2.

The analysis of simulation is consisting of two cases: normal and faulted. The parameters of actuator faults are given in table 3.

A. NORMAL CASE

In the normal case, the actuator system is operated in normal situation. The fault matrix $\Lambda = I^{7\times7}$. Figure 2 shows the output tracking results in the normal case for both BFSMC

TABLE 3. Parameters of actuator faults.

Fault case	Parameters of actuator faults
Normal case	$K = I^{7\times7}$
1st fault Case	$k_2 = \begin{cases} 1, & time < 10s \\ 0, & time \geq 10s \end{cases}$ $k_3 = \begin{cases} 1, & time < 10s \\ 0, & time \geq 10s \end{cases}$
2st fault Case	$k_2 = \begin{cases} 1, & time < 10s \\ 0, & time \geq 10s \end{cases}$ $k_3 = \begin{cases} 1, & time < 10s \\ 0, & time \geq 10s \end{cases}$ $\bar{u} = \begin{cases} 0, & time < 10s \\ -0.1rad, & time \geq 10s \end{cases}$

and ANFTC. The solid lines represent the simulation results of the ANFTC, the dashed lines represent the BFSMC, and the dot lines represent the desired signals. The results show that both methods have similar responses: the output signals could accomplish the asymptotic tracking for the references. It proves the validity of the upper sliding mode controller and the nonlinear feedback CA scheme. Meanwhile, the ANFTC has a faster rate of convergence in sideslip angle tracking which reflects the operation of adaptive module for the uncertainties. Figure 3 displays that the control surfaces deflection signals of the ANFTC will approach constant values when the system is in stable state, and the chattering phenomenon will be effectively suppressed.

B. FAULT CASE

Two types of actuator faults are studied: floating and stuck.

In the first fault case, the right horizontal stabilizer and left ailerons are assumed to have been floating at 10s. The simulation results of the output tracking adopting BFSMC and ANFTC are shown in Figures 4 and 5. Apparently, under the actuators floating fault, ANFTC could maintain stable tracking and overcome the malfunction, however, the BFSMC scheme can not continue to operate normally. By the contrast

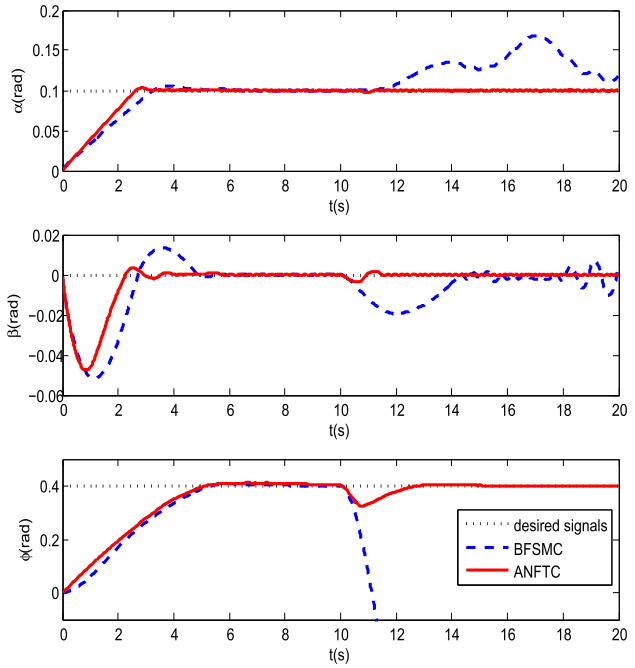

FIGURE 6. Output responses from the BFSMC method (dashed lines) and ANFTC method (solid lines): δ_{re} is floating and δ_{la} is stuck in −0.1 rad at 10s.

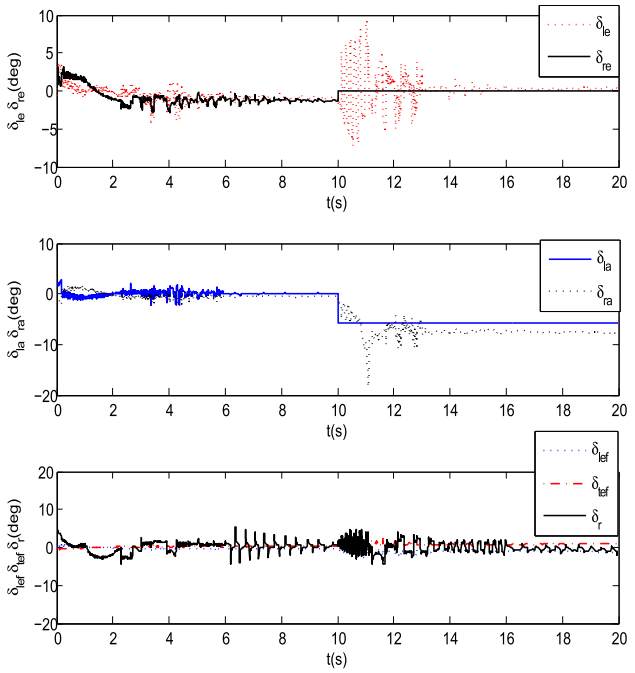

FIGURE 7. Control surfaces deflection signals adopting ANFTC: δ_{re} is floating and δ_{la} is stuck in −0.1rad at 10s.

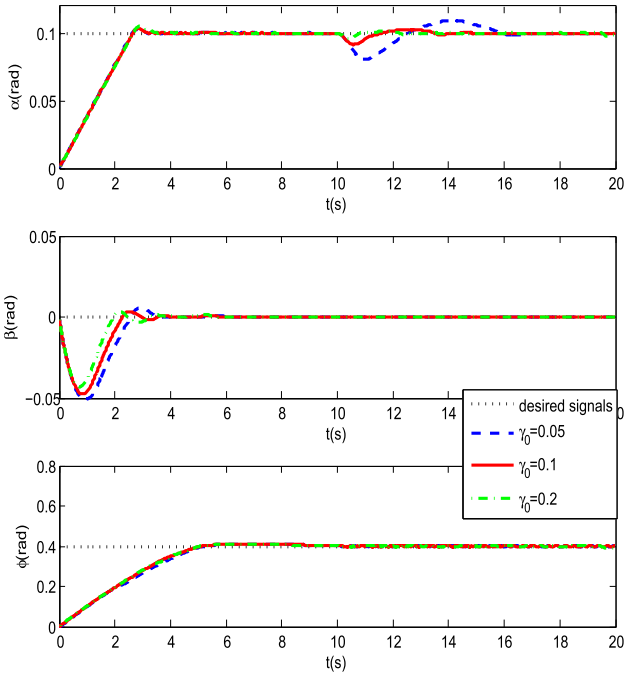

FIGURE 8. Output responses signals adopting ANFTC under the first fault case with different γ_0.

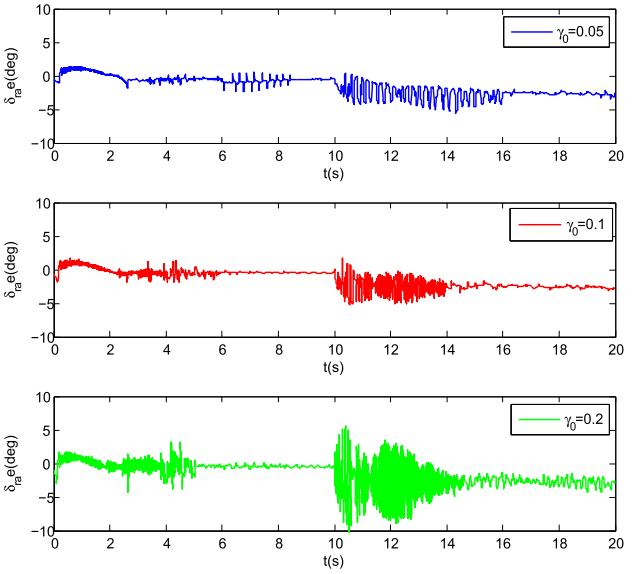

FIGURE 9. Control surfaces deflection signals adopting ANFTC under the first fault case with different γ_0.

of curves, the results support the availability of the ANFTC for tolerating the actuator floating. What's more, the healthy control surfaces would adjust adaptively, and gradually tend to relatively stable states, When the system encounters actuator floating faults.

In the second fault case, the right horizontal stabilizer also maintains floating, but left ailerons is stuck in −0.1rad position at 10s. Figures 6 and 7 show the output tracking curves and control surfaces deflection signals under the second fault case. From the analysis of curves, it explains that the system's stabilities using BFSMC are dissatisfied in the presence of actuator stuck, nevertheless, the controller employing ANFTC can still endure stable states because of the adaptive learning for the information of faults. Through the simulation results, the validity of the proposed ANFTC scheme is fully illustrated.

In addition, in order to illustrate the Remark 2, We choose three different γ_0 parameters to compare the performance of proposed fault-tolerant control system under the first fault case. The control surfaces deflection signals of δ_{ra} and the output tracking curves are provided in Figures 8 and 9. In the Figure 8, the output respond curves display that the response rate and overshoot of the system increase with the increase of parameters both in normal and fault cases. From the Figure 9, When the parameter γ_0 is increased, the frequency of δ_{ra} is accelerated, and the control quantities rise accordingly. These two figures verify the correctness of Remark 2.

V. CONCLUSION

An adaptive closed-loop control allocation based nonlinear FTC scheme has been proposed for an overactuated aircraft with unknown actuator failures. A nonlinear feedback structure integrated with adaptive estimation has been provided to operate control allocation process considering the non-monotonic and the coupled nonlinearities of actuator mapping functions. The proposed adaptive closed-loop control allocation combined with STSMC can tackle the actuator faults such as floating and stuck-in without FDI. The closed-loop stability of the system in the presence of actuator faults has been analyzed. The effectiveness of the proposed approach has been verified through simulation.

REFERENCES

[1] Y. Zhang and J. Jiang, "Bibliographical review on reconfigurable fault-tolerant control systems," *Annu. Rev. Control*, vol. 32, no. 2, pp. 229–252, 2008.

[2] A. A. Amin and K. M. Hasan, "A review of fault tolerant control systems: Advancements and applications," *Measurement*, vol. 143, pp. 58–68, Sep. 2019.

[3] J. Ma, Z. Zheng, and D. Hu, "Modular robust reconfigurable flight control system design for an overactuated aircraft," *IET Control Theory Appl.*, vol. 6, no. 11, pp. 1620–1632, 2012.

[4] B. Xiao, Q. Hu, and P. Shi, "Attitude stabilization of spacecrafts under actuator saturation and partial loss of control effectiveness," *IEEE Trans. Control Syst. Technol.*, vol. 21, no. 6, pp. 2251–2263, Nov. 2013.

[5] M. Chen, B. Jiang, and R. Cui, "Actuator fault-tolerant control of ocean surface vessels with input saturation," *Int. J. Robust Nonlinear Control*, vol. 26, no. 3, pp. 542–564, 2016.

[6] S. Zhao and X. Li, "Prescribed performance fault tolerant control for hypersonic flight vehicles with actuator failures," *IEEE Access*, vol. 7, pp. 100187–100204, 2019, doi: 10.1109/ACCESS.2019.2930658.

[7] X. Yu and J. Jiang, "A survey of fault-tolerant controllers based on safety-related issues," *Annu. Rev. Control*, vol. 39, no. 1, pp. 46–57, Apr. 2015.

[8] S. Yin, B. Xiao, S. X. Ding, and D. Zhou, "A review on recent development of spacecraft attitude fault tolerant control system," *IEEE Trans. Ind. Electron.*, vol. 63, no. 5, pp. 3311–3320, May 2016.

[9] C. De Persis and A. Isidori, "A geometric approach to nonlinear fault detection and isolation," *IEEE Trans. Autom. Control*, vol. 46, no. 6, pp. 853–865, Jun. 2001.

[10] Q. Hu, B. Li, and M. I. Friswell, "Observer-based fault diagnosis incorporating online control allocation for spacecraft attitude stabilization under actuator failures," *J. Astron. Sci.*, vol. 60, no. 2, pp. 211–236, 2013.

[11] W. Chen and M. Saif, "Actuator fault diagnosis for a class of nonlinear systems and its application to a laboratory 3D crane," *Automatica*, vol. 47, no. 7, pp. 1435–1442, 2011.

[12] A. Zolghadri, "Advanced model-based FDIR techniques for aerospace systems: Today challenges and opportunities," *Prog. Aerosp. Sci.*, vol. 53, pp. 18–29, Aug. 2012.

[13] H. Ríos, S. Kamal, L. M. Fridman, and A. Zolghadri, "Fault tolerant control allocation via continuous integral sliding-modes: A HOSM-observer approach," *Automatica*, vol. 51, pp. 318–325, Jan. 2015.

[14] H. An, J. Liu, C. Wang, and L. Wu, "Approximate back-stepping fault-tolerant control of the flexible air-breathing hypersonic vehicle," *IEEE/ASME Trans. Mechatronics*, vol. 21, no. 3, pp. 1680–1691, Jun. 2016.

[15] J. Liu, H. An, Y. Gao, C. Wang, and L. Wu, "Adaptive control of hypersonic flight vehicles with limited angle-of-attack," *IEEE/ASME Trans. Mechatronics*, vol. 23, no. 2, pp. 883–894, Apr. 2018.

[16] Y. Gao, J. Liu, Z. Wang, and L. Wu, "Interval type-2 FNN-based quantized tracking control for hypersonic flight vehicles with prescribed performance," *IEEE Trans. Syst., Man, Cybern., Syst.*, to be published, doi: 10.1109/TSMC.2019.2911726.

[17] T. A. Johansen and T. I. Fossen, "Control allocation—A survey," *Automatica*, vol. 49, no. 5, pp. 1087–1103, 2013.

[18] A. Casavola and E. Garone, "Fault-tolerant adaptive control allocation schemes for overactuated systems," *Int. J. Robust Nonlinear Control*, vol. 20, no. 17, pp. 1958–1980, 2010.

[19] O. Harkegard, "Efficient active set algorithms for solving constrained least squares problems in aircraft control allocation," in *Proc. IEEE Conf. Decis. Control*, Dec. 2002, pp. 1295–1300.

[20] M. Bodson and S. A. Frost, "Load balancing in control allocation," *J. Guid., Control, Dyn.*, vol. 34, no. 2, pp. 380–387, 2011.

[21] A. K. Naskar, S. Patra, and S. Sen, "Reconfigurable direct allocation for multiple actuator failures," *IEEE Trans. Control Syst. Technol.*, vol. 23, no. 1, pp. 397–405, Jan. 2015.

[22] T. A. Johansen, "Optimizing nonlinear control allocation," in *Proc. IEEE Conf. Decis. Control*, Nassau, Bahamas, Dec. 2004, pp. 3435–3440.

[23] V. Poonamallee, S. Yurkovich, A. Serrani, D. Doman, and M. Oppenheimer, "Dynamic control allocation with asymptotic tracking of time-varying control trajectories," in *Proc. Amer. Control Conf.*, 2004, pp. 2098–2103.

[24] M. W. Leonard, "Real-time optimization for use in a control allocation system to recover from pilot induced oscillations," in *Proc. AIAA Guid., Navigat., Control Conf.*, Boston, MA, USA, 2013, p. 5239.

[25] B. Wang and Y. Zhang, "An adaptive fault-tolerant sliding mode control allocation scheme for multirotor helicopter subject to simultaneous actuator faults," *IEEE Trans. Ind. Electron.*, vol. 65, no. 5, pp. 4227–4236, May 2018.

[26] R. Galván-Guerra, X. Liu, S. Laghrouche, L. Fridman, and M. Wack, "Fault-tolerant control with control allocation for linear time varying systems: An output integral sliding mode approach," *IET Control Theory Appl.*, vol. 11, no. 2, pp. 245–253, 2017.

[27] H. Gui and A. H. J. de Ruiter, "Adaptive fault-tolerant spacecraft pose tracking with control allocation," *IEEE Trans. Control Syst. Technol.*, vol. 27, no. 2, pp. 479–494, Mar. 2019.

[28] Q. Hu, B. Li, D. Wang, and E. K. Poh, "Velocity-free fault-tolerant control allocation for flexible spacecraft with redundant thrusters," *Int. J. Syst. Sci.*, vol. 46, no. 6, pp. 976–992, 2015.

[29] J. Ma, X. Lu, Z. Zheng, and D. Hu, "Differential evolution strategy for over-actuated control allocation problem with nonmonotonic nonlinearities," in *Proc. Eur. Control Conf.*, Budapest, Hungary, Aug. 2009, pp. 585–590.

[30] M. Chen, "Constrained control allocation for overactuated aircraft using a neurodynamic model," *IEEE Trans. Syst., Man, Cybern., Syst.*, vol. 46, no. 12, pp. 1630–1641, Oct. 2016.

[31] Y. Yang and Z. Gao, "A new method for control allocation of aircraft flight control system," *IEEE Trans. Autom. Control*, to be published, doi: 10.1109/TAC.2019.2918122.

[32] L. Cui, Z. Zuo, and Y. Yang, "A control-theoretic study on iterative solution to control allocation for over-actuated aircraft," *IEEE Trans. Syst., Man, Cybern., Syst.*, to be published, doi: 10.1109/TSMC.2019.2924357.

[33] B. Choi, H. J. Kim, and Y. Kim, "Robust control allocation with adaptive backstepping flight control," *Inst. Mech. Eng., G, J. Aerosp. Eng.*, vol. 228, no. 7, pp. 1033–1046, 2014.

[34] S. P. Bhat and D. S. Bernstein, "Finite-time stability of continuous autonomous systems," *SIAM J. Control Optim.*, vol. 38, no. 3, pp. 751–766, Jan. 2000.

[35] H. Khalil, *Nonlinear Systems*, 3rd ed. Upper Saddle River, NJ, USA: Prentice-Hall, 2002.

[36] P. Li, J. Ma, and Z. Zheng, "Robust adaptive sliding mode control for uncertain nonlinear MIMO system with guaranteed steady state tracking error bounds," *J. Franklin Inst.*, vol. 353, pp. 303–321, Jan. 2016.

[37] J. Ma, S. S. Ge, Z. Zheng, and D. Hu, "Adaptive NN control of a class of nonlinear systems with asymmetric saturation actuators," *IEEE Trans. Neural Netw. Learn. Syst.*, vol. 26, no. 7, pp. 1532–1538, Jul. 2015.

[38] J. Ma, Z. Zheng, and P. Li, "Adaptive dynamic surface control of a class of nonlinear systems with unknown direction control gains and input saturation," *IEEE Trans. Cybern.*, vol. 45, no. 4, pp. 728–741, Apr. 2015.
[39] W. Durham, "Efficient, near-optimal control allocation," *J. Guid., Control, Dyn.*, vol. 22, no. 2, pp. 369–372, 1999.
[40] X. Qu, "Tailless flying wing aircraft multi-control surfaces control allocation technology research," Ph.D. dissertation, Northwestern Polytechnical Univ., Xi'an, China, 2015, pp. 105–107.
[41] X. Yu and O. Kaynak, "Sliding-mode control with soft computing: A survey," *IEEE Trans. Ind. Electron.*, vol. 56, no. 9, pp. 3275–3285, Sep. 2009.
[42] R. Beck, "Application of control allocation methods to linear systems with four or more objectives," Ph.D. dissertation, Dept. Aerosp. Eng., Virginia Polytech. Inst. State Univ., Blacksburg, VA, USA, 2002.

BINWEN LU received the B.E. and M.E. degrees in control science and engineering from Naval Aeronautical University, Yantai, China, in 2012 and 2014, respectively. He is currently pursuing the Ph.D. degree with the College of Intelligent Science Technology, National University of Defense Technology, Changsha, China. His research interest includes fault tolerant flight control.

JIANJUN MA (M'11) received the M.E. and Ph.D. degrees in control science and engineering from the National University of Defense Technology, Changsha, China, in 2004 and 2010, respectively. From 2011 to 2012, he was a Research Fellow with the Interactive Digital Media Institute (IDMI), National University of Singapore, Singapore. He is currently an Associate Professor with the College of Intelligent Science and Technology, National University of Defense Technology. His research interests include guidance and control of aerospace vehicles, cooperative control theory, and fault tolerant flight control.

ZHIQIANG ZHENG received the Ph.D. degree in aerospace engineering from the University of Liege, Liege, Belgium, in 1994. He is currently a Professor with the College of Intelligent Science and Technology, National University of Defense Technology, Changsha, China. His research interests include precision guidance and control, multirobot coordination control, and so on.